Concentration effects on peptide elution from pendant PEO layers

Citation	Wu, X., Ryder, M. P., McGuire, J., & Schilke, K. F. (2014). Concentration effects on peptide elution from pendant PEO layers. Colloids and Surfaces B: Biointerfaces, 118, 210-217. doi:10.1016/j.colsurfb.2014.03.056
DOI	10.1016/j.colsurfb.2014.03.056
Publisher	Elsevier
Version	Accepted Manuscript
Terms of Use	http://cdss.library.oregonstate.edu/sa-termsofuse

Concentration effects on peptide elution from pendant PEO layers

Xiangming Wu, Matthew P. Ryder, Joseph McGuire, Karl F. Schilke*

School of Chemical, Biological and Environmental Engineering, Oregon State University, Corvallis, OR 97331

* Corresponding Author:

Gleeson Hall Rm. 102
Oregon State University
Corvallis, OR 97331 USA
E-mail: *karl.schilke@oregonstate.edu*
FAX: 1-541-737-4600
Telephone: 1-541-737-7283

Abstract

In earlier work, we have provided direction for development of responsive drug delivery systems based on modulation of structure and amphiphilicity of bioactive peptides entrapped within pendant polyethylene oxide (PEO) brush layers. Amphiphilicity promotes retention of the peptides within the hydrophobic inner region of the PEO brush layer. In this work, we describe the effects of peptide surface density on the conformational changes caused by peptide-peptide interactions, and show that this phenomenon substantially affects the rate and extent of peptide elution from PEO brush layers. Three cationic peptides were used in this study: the arginine-rich amphiphilic peptide WLBU2, the chemically identical but scrambled peptide S-WLBU2, and the non-amphiphilic homopolymer poly-*L*-arginine (PLR). Circular dichroism (CD) was used to evaluate surface density effects on the structure of these peptides at uncoated (hydrophobic) and PEO-coated silica nanoparticles. UV spectroscopy and a quartz crystal microbalance with dissipation monitoring (QCM-D) were used to quantify changes in the extent of peptide elution caused by those conformational changes. For amphiphilic peptides at sufficiently high surface density, peptide-peptide interactions result in conformational changes which compromise their resistance to elution. In contrast, elution of a non-amphiphilic peptide is substantially independent of its surface density, presumably due to the absence of peptide-peptide interactions. The results presented here provide a strategy to control the rate and extent of release of bioactive peptides from PEO layers, based on modulation of their amphiphilicity and surface density.

Keywords

peptide elution; PEO brush; WLBU2; cationic amphiphilic peptides; polyarginine; circular dichroism (CD); α-helix; coiled-coils

Introduction

In an earlier paper [1], we used circular dichroism (CD) to evaluate the structures of poly-*L*-arginine (PLR) and the cationic, amphiphilic peptide (CAP) WLBU2 in pendant PEO layers, as well as the reversibility of peptide location in such layers with changing solvent conditions. Those results indicated that some minimal degree of structural order (α-helix) is necessary for peptide entry into the PEO layer, and that peptide location within the hydrophobic inner region of the PEO brush may result in a cooperative increase in α-helix content. In addition, while peptide interaction with the PEO chains resulted in entrapment and conformational change that was irreversible to elution with changing solution conditions in the case of WLBU2, the adsorption and conformational change of the non-amphiphilic PLR was reversible.

Current work underway in our laboratory features the sequential and competitive adsorption behavior of peptides, including WLBU2 and PLR, at pendant PEO brush layers. In sequential adsorption experiments it is necessary to vary surface density of the first peptide introduced to the layer in order to properly interpret its replacement by the second peptide introduced. We determined during the course of these experiments that our previous conclusion of entrapment and conformational change being irreversible to elution for the amphiphilic WLBU2 was contextual, being valid only when its surface density is sufficiently low. Our objectives with this paper are to establish an improved understanding of surface density effects on peptide elution from PEO layers, and to provide evidence of concentration-dependent, peptide-peptide interactions likely contributing to those effects. The adsorption behavior of three peptides was evaluated for this purpose, including, in addition to WLBU2 and PLR, a peptide chemically identical to WLBU2 but of scrambled sequence (S-WLBU2).

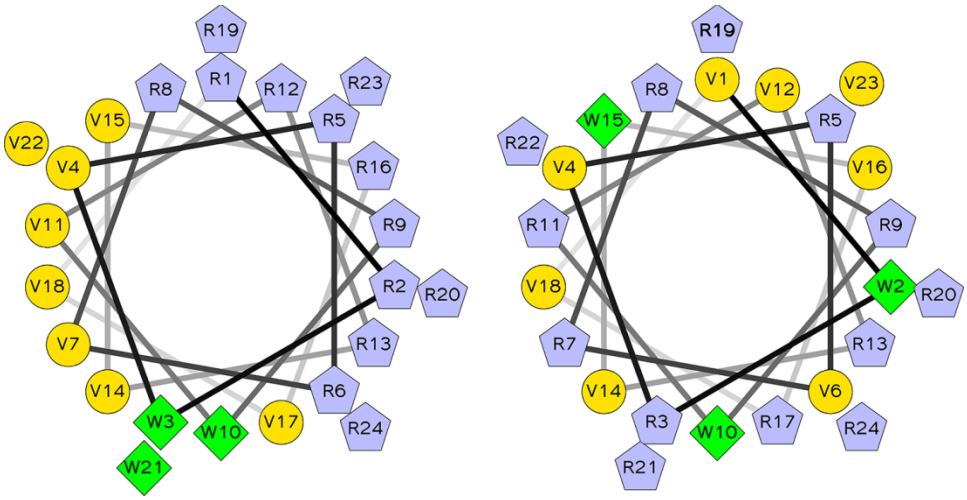

Figure 1. Helix wheel representations of WLBU2 (left), with face-segregation of positively-charged Arg residues on the α-helix, and S-WLBU2 (right) which has uniformly distributed charge.

WLBU2 is a synthetic, 24-residue CAP with 13 positively charged arginine residues, and 11 non-polar valine or tryptophan residues. It shows substantial promise for clinical applications, due to its wide spectrum antimicrobial activity against both Gram-negative and Gram-positive bacteria under physiological conditions [2-8]. The structure of WLBU2 in water is substantially disordered, but the peptide gains considerable secondary structure, involving segregation of its positively-charged and hydrophobic groups onto opposing faces of an α-helix, in the presence of counterions, membrane-mimetic solvents, or bacterial membranes. Moreover, WLBU2 retains its antimicrobial activity when immobilized at solid surfaces by a number of methods [2, 6-8]. While chemically identical to WLBU2, the scrambled sequence of S-WLBU2 eliminates the ordered segregation of positively-charged and hydrophobic residues of WLBU2 during helix formation (Figure 1), and is associated with a very low hydrophobic moment in comparison to WLBU2 (0.1 vs. 10.7, respectively). PLR is chemically homogeneous and not amphiphilic. When dissolved in water under neutral pH, PLR adopts a combination of random coil and extended structures (e.g. polyproline-II and 2.5_1 helix), while both WLBU2 and S-WLBU2 show

a random coil structure [1, 3-5, 9-13]. An α-helical conformation can be achieved in all three peptides by addition of perchlorate ions (ClO_4^-) [12].

Biocompatible, drug-loaded surface coatings based on entrapment of bioactive agents show great promise in enhancing the safety and performance of relatively short-term medical device applications (e.g., anti-infective coatings for acute hemodialysis catheters), as well as utility in blood processing (e.g., sepsis treatment) using high surface-to-volume ratio, high flow rate, extracorporeal microfluidic devices. Moreover, entrapment of therapeutic peptides may also support novel drug delivery strategies (e.g., PEO-coated nanoparticle carriers) that can potentially overcome barriers to oral delivery of peptide drugs **[14]**. It has been shown that surface modification using PEO can improve the biocompatibility and extend the circulation time of nanoparticle drug carriers **[15, 16]**. Peptides which are entrapped in PEO brushes are protected from competitive elution by large blood proteins (e.g. fibrinogen) without compromising their protein repulsion **[17, 18]**. In addition, the rate and extent of peptide release from PEO brushes can be controlled by modulation of the peptide surface density and amphiphilicity, potentially eliminating burst release effects which are common with nanocarriers of large surface area **[19, 20]**.

Materials and Methods

Peptides and materials. **S**ynthetic poly-*L*-arginine hydrochloride (PLR, n ≈ 30, M_n = 5.8 kDa, PDI < 1.20) was purchased from Alamanda Polymers (Huntsville, AL). The 24-residue peptides WLBU2 (RRWVRRVRRWVRRVVRVVRRWVRR, 3.4 kDa) and the scrambled sequence S-WLBU2 (VWRVRVRRRWRVRVWVRVRRRRVR) were purchased from Genscript (Piscataway, NJ). All peptides were used without further purification. Stock solutions of each peptide at 5 mg/mL in HPLC water were frozen in 1 mL aliquots, which were thawed and then

diluted immediately before use to 0.2 mg/mL in 0.2 M $HClO_4$ (to induce α-helical conformation). Diluted peptide solutions were degassed under vacuum immediately before use.

Self-assembled PEO brush layers were formed by suspension of hydrophobic silica nanoparticles (R816, Degussa, 190 m^2/g, 10-12 nm) in Pluronic® F108 (BASF) in HPLC water for 10 h on a rotator. The expected surface coverage of F108 is about 3.3 mg/m^2 [21, 22]; a 5× excess of F108 over this amount was used to ensure good coverage of the nanoparticles (NPs). Prior to contacting peptides, F108-coated NPs were rinsed with HPLC water by centrifugation twice (10000 rpm, 20 min) in order to remove excess F108. Uncoated and F108-coated NPs were then incubated with PLR, WLBU2 or S-WLBU2 (0.2 mg/mL in 0.2 M $HClO_4$) for 2 h at 20 °C. The concentration of NPs was varied from 1 to 10 mg/mL to provide different available surface areas for peptide adsorption.

Evaluation of peptide structure and elutability. Peptide secondary structure, in the presence or absence of nanoparticles, was evaluated by circular dichroism (CD) using a Jasco J-815 spectropolarimeter (Easton, MD) at 25 °C. The spectra from each of three replicates for each sample exhibited only slight (~5%) differences in signal intensity; representative spectra are thus shown throughout. The instrument was calibrated with 0.6 mg/mL *D*(+)-camphorsulfonic acid. Spectra were recorded from 185 to 260 nm in 0.5 nm increments (0.1 cm path length), with 5 scans recorded and averaged in order to increase the signal-to-noise ratio. All peptide solutions were filtered (0.20 μm) prior to contact with NPs and recording of CD spectra. All spectra were blanked against peptide-free solutions.

After the CD measurements, the peptide-NP suspensions from each of three replicates were rinsed by centrifugation (10,000 rpm, 20 min) and resuspension in water; this process was

repeated twice to remove excess peptide. The amount of peptide removed in each of the supernatants from the NPs was then quantified by UV spectrophotometry against the original peptide solutions at 230 nm (for PLR) or 280 nm (for WLBU2 and S-WLBU2), and the total eluted peptide calculated from this data. The UV absorbance from each of the three replicates for each sample were nearly identical, with negligible (~3%) differences in signal intensity; representative data are shown throughout.

Preparation of QCM-D sensors. QSX303 silicon dioxide QCM-D sensors (Q-Sense, Linthicum, MD) were cleaned according to manufacturer's protocol: 10 min UV/ozone treatment followed by immersion in 2% sodium dodecyl sulfate (SDS) for 30 min, and a 10 min rinse with HPLC water. After cleaning, sensors were dried under a stream of nitrogen and placed in the UV/ozone chamber again for 10 min.

The sensor surfaces were then modified by vapor deposition of trichlorovinylsilane (TCVS, TCI America, Portland, OR). 200 µL of TCVS was evaporated at 20 °C into a stream of dry nitrogen carrier gas, which was directed over the sensor surfaces for 4 h. The silanized, hydrophobic sensors were then incubated overnight with 5% Pluronic® F108 in water, and then γ-irradiated to 0.3 Mrad to covalently attach the F108 to the surface [21, 23]. The irradiated sensors were rinsed with water, dried with nitrogen, and stored in the dark to avoid oxidation of the vinyl moieties.

Measurement of the rate and extent of peptide adsorption and elution. The adsorption and elution of peptides were measured with a Q-Sense E4 QCM-D (Q-sense, Linthicum, MD). QCM-D allows simultaneously measuring changes in resonance frequency (ΔF) and energy dissipation (ΔD) of QCM-D sensors. Sample solutions were pumped across F108-coated silica

sensors at 100 µL/min, and the sample stage was held at 25 °C. QCM-D experiments began with a baseline of peptide-free 0.2M $HClO_4$, followed by introduction of 0.1 mg/mL or 0.005 mg/mL peptide in 0.2M $HClO_4$, and a subsequent rinse with water. Adsorption and elution steps were each allowed to proceed for 40 min. All QCM-D experiments were conducted in triplicate. Reproducibility of QCM-D measurements is high, typically with less than 5% variation was observed in the plateau ΔF and ΔD at each adsorption/rinse step. Representative data are shown throughout.

Results and Discussion

Relationship between peptide surface density and peptide elution from PEO layers. Peptide concentration at PEO-coated nanoparticle surfaces was varied by altering nanoparticle concentration (from 1 to 10 mg/mL) in peptide-nanoparticle suspensions with constant peptide concentration (0.2 mg/mL). More than 95% of the dissolved peptide was entrapped in every suspension tested, corresponding to peptide surface densities ranging from about 0.02 to 0.2 molecules/nm^2. The elutability of each peptide recorded after contact with peptide-free water is plotted against peptide surface density in Figure 2.

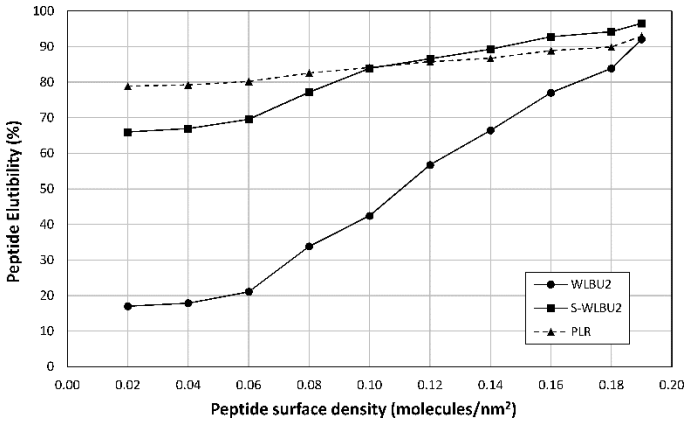

Figure 2. Effect of surface peptide density on elutability of WLBU2, S-WLBU2 and PLR from F108-coated nanoparticles.

As shown in Figure 2, entrapped WLBU2 showed a substantially greater concentration dependence on elution than shown by entrapped S-WLBU2 or PLR. The high resistance to elution at low peptide surface density is consistent with our earlier report and attributed to association of the amphiphilic WLBU2 with PEO chain segments in the hydrophobic inner region of the brush [1, 21, 24]. The elutability of S-WLBU2 and PLR was less strongly affected by the peptide surface density, and both were more elutable than WLBU2 at all but the highest surface density tested.

S-WLBU2, while comprised of the same amino acids and carrying the same +13 charge as WLBU2, features arginine residues alternating with valine or tryptophan to distribute the positive charge uniformly around the α-helix (Figure 1). The tryptophan residues are also distributed along the full length of the peptide. S-WLBU2 was designed to have a very low hydrophobic moment, and these attributes are consistent with its elution from the PEO layer being greater than that recorded for WLBU2 at low peptide surface densities. The non-amphiphilic PLR is highly elutable from PEO layers (Figure 2), which is consistent with our earlier work using CD and optical waveguide lightmode spectroscopy [1]. The total absence of hydrophobic residues and the abundant positive charges on all sides of PLR lead to electrostatic repulsion among peptides within the brush, as well as making PLR highly soluble in water. In fact, the elutability of PLR is only slightly dependent on its surface density (Figure 2).

WLBU2 and S-WLBU2 both exhibit substantially increased elutability at high peptide surface densities (i.e. low nanoparticle concentrations). It is fair to expect that this high elutability is due to intermolecular interactions, which interfere with the stable hydrophobic association of the individual peptides within the brush, or otherwise promote their enhanced solubility in water.

WLBU2 is highly α-helical in $HClO_4$, and its entrapment in PEO is accompanied by a further increase in its helicity [1]. Upon sufficiently close approach, peptides like WLBU2 which possess an amphiphilic-segregated α-helical conformation are able to form *α*-helical, "coiled-coil" conformations. These structures, which are comprised of two or more intertwined α-helical chains, are stabilized through multiple interchain hydrophobic interactions [25]. For example, Zhou *et al*. produced a two-stranded *α*-helical coiled-coil consisting of two identical 35-residue polypeptides. The peptides were designed with polar (lysine and glutamic acid) and non-polar (leucine and alanine) residues distributed on average 3.5 residues apart, in order to form face-segregated amphiphilic *α*-helices. These synthetic peptides spontaneously self-assembled into coiled-coil structures in physiological conditions [26, 27]. WLBU2 has a very similar distribution of polar and nonpolar residues, and is thus also expected to form *α*-helical coiled-coil structures at sufficiently high concentration. Such coiled-coils may consist of two or more peptides [25, 28], and in the case of WLBU2 would likely feature a hydrophobic interior, with an exterior dominated by positively-charged arginine groups. Such a coiled-coil structure would be expected to behave very similarly to the highly cationic but non-amphiphilic PLR, in terms of its interaction with the PEO brush (shown schematically in Figure 3). The presumed "standing-up" peptide orientation depicted is based on steric hindrance between the WLBU2 *α*-helix (about 1.6 by 4.5 nm, including side chains) and the pendant PEO chains spaced ~2 nm apart. The coiled-coil conformations are even bulkier and more uniformly charged, and thus are even less likely to be able to "lie down" on the surface.

With respect to S-WLBU2, it has been shown [29, 30] that peptides with alternating hydrophobic and polar residues are able to self-assemble into stable β-sheet conformations. It is reasonable to expect that, as favorable peptide-PEO interactions which hold entrapped peptides in place give

way at high surface densities to peptide-peptide associations, the peptides become more elutable as the population of coiled-coils increases.

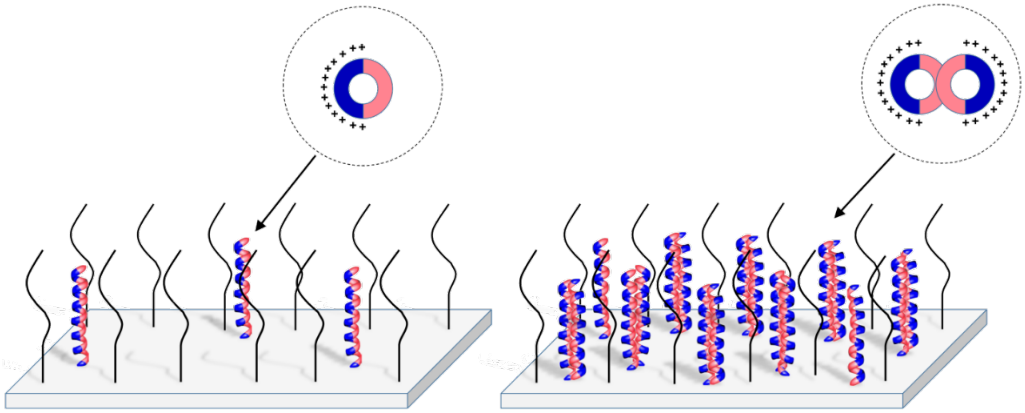

Figure 3. Speculative schematic representation of WLBU2 as single-stranded amphiphilic α-helices at low peptide surface density (left), and formation of less-amphiphilic α-helical coiled-coil structures at high peptide surface density (right). Figure not to scale.

Surface density effects on peptide structure in PEO layers. No conformational change was observed for WLBU2, S-WLBU2 and PLR in aqueous solutions of F108, indicating that peptide conformation is largely unaffected by the presence of free F108 triblocks [1]. Formation of coiled-coil or other structures associated with increasing peptide surface density and elutability should be detectable by specific changes in the CD signal. The surface density of peptides at uncoated (hydrophobic) and PEO-coated nanoparticle surfaces was varied as above, by altering the nanoparticle concentration (from 1 to 10 mg/mL) in peptide-nanoparticle suspensions with constant peptide concentration (0.2 mg/mL). CD spectra were acquired for WLBU2 in contact with uncoated or PEO-coated nanoparticles at different peptide surface densities (Figure 4).

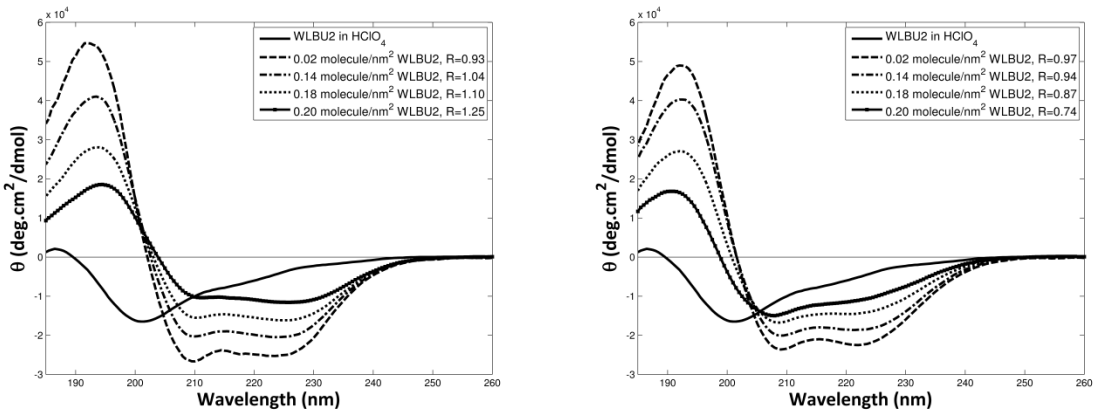

Figure 4. CD spectra of WLBU2 in 0.2M $HClO_4$ at different peptide surface densities on F108-coated (left) and uncoated (right) NPs.

The CD spectrum of an α-helix typically exhibits a maximum at 193 nm, and two minima at 208 and 222 nm. An increase in the magnitude of ellipticity at 222 nm for a given sample is associated with an increase in α-helix content [31, 32]. Deconvolution of these CD spectra with DichroWeb [33, 34] indicate that WLBU2 in 0.2 M $HClO_4$ exhibits 17% α-helicity. In the presence of F108-coated nanoparticles at 1, 2, 4 and 10 mg/mL (corresponding to decreasing peptide surface densities of 0.20, 0.18, 0.14 and 0.02 molecules/nm^2), the helicity of WLBU2 was increased to 50, 65, 84 and 95%, respectively. The increase in helicity is due to promotion of hydrogen-bonding along the peptide backbone, which accompanies the change in microenvironment caused by location within the hydrophobic interior of the PEO layer [1, 5, 24]. Interference with this intra-chain hydrogen-bonding by neighboring peptides is presumably responsible for the reduction in α-helix content observed at increased peptide surface densities (Figure 4, left panel).

While the ellipticity at 222 nm is primarily responsive to the α-helix content, the minimum at 208 nm is itself sensitive to helix-helix interactions [27, 35]. In fact, CD has been applied extensively to the study of the formation of α-helical, coiled-coil structures [35-39]. In particular,

the ratio, *R*, of the ellipticities at 222 nm and 208 nm can be used to distinguish coiled-coils from single-stranded α-helices. Typically, a value of $R > 1$ (i.e. $\theta_{222\ nm} > \theta_{208\ nm}$) is associated with coiled-coil structures, while a value of $R \leq 1$ is indicative of single-stranded α-helices [35-39]. WLBU2 exhibits a large amount of predominantly single-stranded α-helix structure ($R = 0.93$) on F108-coated nanoparticles at a surface density of 0.02 peptides/nm^2 (dashed line in Figure 4, left panel). This suggests that at sufficiently low peptide surface density, peptides exist mainly as single α-helical molecules (Figure 3, left). As the surface density of peptides increases, the ratio *R* increases to values greater than unity, indicating the formation of a substantial number of α-helical coiled-coil structures (Figure 3, right) [36-39].

While the CD spectra of WLBU2 adsorbed at uncoated, hydrophobic nanoparticles (Figure 4, right panel) indicate an increase in α-helicity, especially at low peptide surface density, there is no evidence of α-helical coiled-coils, as $R < 1$ at all of the surface densities tested. The increase in peptide helicity is likely due to the preferential association of the non-polar Val/Trp residues with the hydrophobic surface, which promotes the segregation of polar and non-polar residues onto opposing sides of the peptide and stabilizes the α-helix [21]. Electrostatic repulsion by the positively-charged Arg residues on the solvent-exposed helix face would make formation of coiled-coil structures unfavorable, even if the peptide surface density were high. However, peptides which are entrapped within a PEO brush apparently do not directly interact with the underlying surface [23]. Thus, WLBU2 peptides entrapped in a PEO brush still form highly-charged coiled-coil structures, with low resistance to elution, at sufficiently high surface density.

Similarly to WLBU2, the CD spectra of S-WLBU2 in suspension with PEO-coated nanoparticles (Figure 5, left panel) indicate a substantial gain (from 17 to 89%) in α-helix content after entering the brush, when the surface density is low (0.02 peptides/nm^2). However, with

increasing peptide surface density, the structure adopted by the peptide becomes β-sheet rather than α-helical coiled-coils. The CD spectra of peptides with β-sheet conformation usually have a single minimum between 210 and 220 nm, and a single maximum between 195 and 200 nm, and overall intensities much lower than the minima consistent with α-helices [31, 32]. Deconvolution of the spectra with DichroWeb indicate that S-WLBU2 exhibits 31% β-sheet and 53% α-helix structure at a surface density of 0.14 peptides/nm^2, has 54% β-sheet and 16% α-helix at 0.18 peptides/nm^2, and reaches 67% β-sheet with only negligible α-helix (3%) at 0.20 peptides/nm^2. The amino acid sequence of S-WLBU2 is not conducive to formation of face-segregated amphiphilic α-helices (Figure 1); instead, the peptide likely extends into β-strands, isolating the alternating non-polar residues onto one side of the sheet [30]. At sufficiently high peptide surface densities, these β-strands may self-assemble into stable β-sheet structures stabilized by inter-chain hydrogen-bonding and hydrophobic interactions [40].

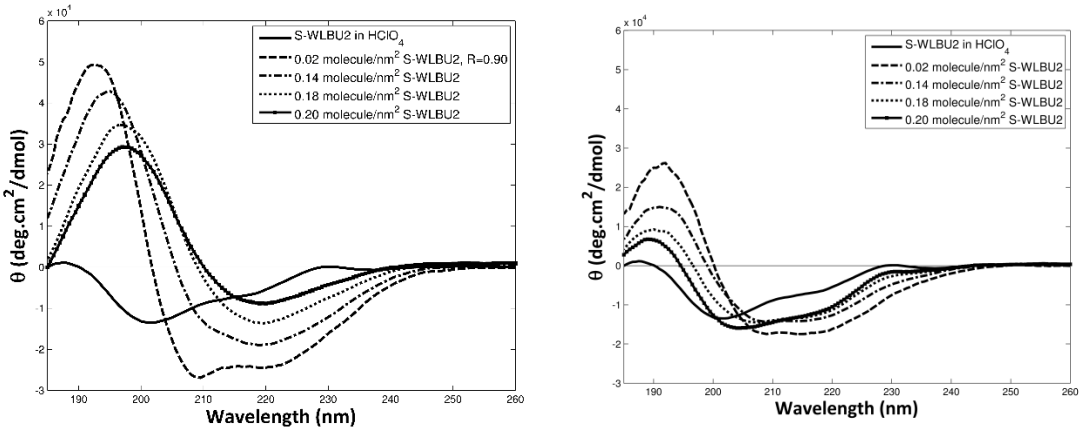

Figure 5. CD spectra of S-WLBU2 in 0.2M $HClO_4$ at different peptide surface densities on F108-coated **(left)** and uncoated (right) NPs.

The effects of peptide concentration on the conformation of adsorbed S-WLBU2 are less obvious at uncoated, hydrophobic surfaces than at PEO-coated surfaces (Figure 5, right panel). While S-WLBU2 in a PEO brush was almost completely α-helical (89%) at the lowest peptide surface

density (0.02 peptides/nm^2), the same peptide adopts a substantial β-sheet structure (30%) on the uncoated, hydrophobic surface. Interactions between the hydrophobic surface and the alternating, non-polar residues of S-WLBU2 likely result in extension of the peptide chain, thus favoring β-sheet formation on the surface. Increasing the surface density of S-WLBU2 appears only to increase the number of layers of β-sheet, as no major conformational change is associated with increasing peptide density (Figure 5, right panel).

Unlike WLBU2 and S-WLBU2, PLR is a non-amphiphilic homopolymer with positive charges which uniformly surround the α-helix. Accordingly, electrostatic repulsions are expected to prevent peptide-peptide interactions, even at high surface density. CD spectra show that the helicity of PLR in 0.2 M $HClO_4$ solution is 55%, and is increased to 65% after contact with a PEO layer (Figure 6, left). Changes in surface density have little or no further effect on the conformation of PLR, whether on PEO-coated or uncoated hydrophobic surfaces (Figure 6).

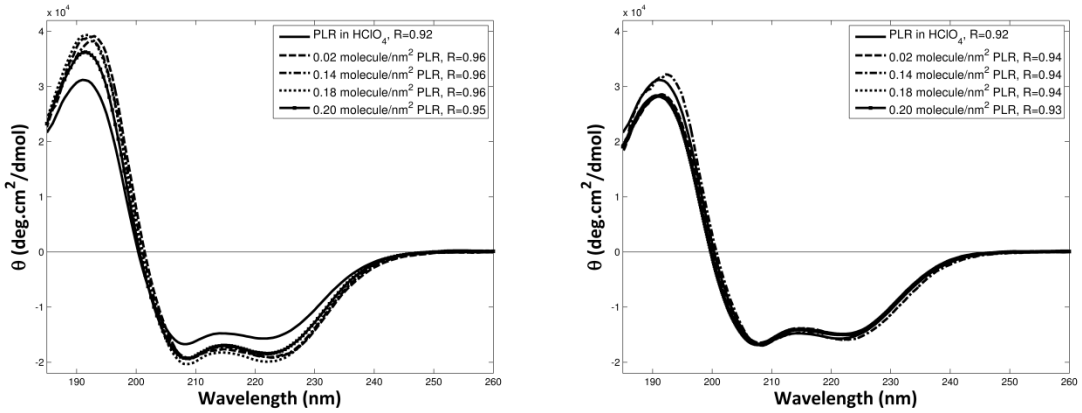

Figure 6. CD spectra of PLR in 0.2M $HClO_4$ at different peptide surface densities on F108-coated (left) and uncoated (right) NPs.

The structures of WLBU2, S-WLBU2 and PLR at different peptide density in the PEO layer are summarized in Table 1. In summary, interactions between peptide molecules within the PEO brush layer are highly dependent on the properties of the peptide, specifically amphiphilicity,

distribution of polar and non-polar residues, and charge. Elution of an amphiphilic peptide from the PEO brush layer is significantly affected by its surface density, while elution of a non-amphiphilic peptide is substantially independent of surface density. This difference in elution behavior is attributed to peptide-peptide interactions in the former case and the absence of such interactions in the latter.

Table 1. The structure of WLBU2, S-WLBU2 and PLR at different peptide surface density on F108-coated NPs.

	Peptide structure		
Peptide surface density	WLBU2	S-WLBU2	PLR
Low	Single α-helices	Single α-helices	Single α-helices
High	α-helical coiled-coils	β-sheets	Single α-helices

Direct detection of peptide adsorption and elution at covalently immobilized PEO layers. We used QCM-D to measure the effect of surface concentration on the rate and extent of peptide elution. Figure 7 shows the representative changes in resonant frequency (ΔF) and viscous dissipation (ΔD) upon adsorption and elution of peptides from F108-coated silica sensors [41, 42]. The decrease in frequency (indicative of an increase in adsorbed mass) upon introduction of WLBU2 to F108-coated sensors at a peptide concentration of 0.1 mg/mL was about three times greater than that recorded for WLBU2 at 0.005 mg/mL (Figure 7, top panels). Upon elution, the frequency change indicated rapid and substantially complete removal of WLBU2 from the PEO brush that had been introduced at 0.1 mg/mL. However, a much slower, and only partial, removal of WLBU2 was observed when the peptide had been introduced at 0.005 mg/mL. These results are consistent with the greater resistance to elution by peptides at low surface density within the brush observed on nanoparticles (Figure 2).

Modeling of the frequency and dissipation data of Figure 7, in order to determine the adsorbed mass and effective layer viscosity, could not be performed with good certainty, as neither the Sauerbrey equation nor the Voigt model are appropriately applied in this context. The Sauerbrey equation should only be used with relatively uniform, rigid, thin films that show negligible dissipation change, while the Voigt model did not successfully calculate adsorbed mass from a simultaneous decrease in frequency and dissipation [43, 44]. Qualitatively, however, the frequency and dissipation patterns in Figure 7 (top panel) likely represent the incorporation of WLBU2 into an initially "soft" dissipative surface (i.e. a pendant PEO layer, as opposed to a solid surface), and a concomitant increase in the layer stiffness. In comparison, a decrease in layer stiffness (i.e. increased viscoelasticity) is associated with protein adsorption on a rigid surface, suggesting that the observed frequency change was not due to adsorption of WLBU2 at "bare spots" in the brush. In contrast, the changes in resonant frequency (ΔF) for S-WLBU2 indicate a rapid and nearly complete removal of the peptide, whether originally introduced at high or low concentrations (Figure 7, bottom panels). This suggests that elution of the scrambled peptide is much less affected by its concentration at the surface than the face-segregated α-helix formed by WLBU2. Using optical waveguide lightmode spectroscopy (OWLS), we have observed that, like S-WLBU2, the non-amphiphilic PLR remains completely elutable from a PEO brush, even at very low surface peptide density [1].

Interestingly, the dissipation recorded during the adsorption of S-WLBU2 at high concentration decreased rapidly at first, then slowly increased (Figure 7, bottom left). An increase in the dissipation is associated with decreases in the stiffness of the adsorbed layer. Such a change would be consistent with a slow conformational change undergone by S-WLBU2 at the interface. Presumably, S-WLBU2 retains the α-helix structure induced by perchlorate ion during the initial

adsorption, but rearranges to a β-sheet conformation as the peptide concentration in the PEO layer becomes sufficiently high. This is also consistent with recent reports that α-helical peptide layers adsorbed on gold QCM-D sensors are more rigid than peptide layers adsorbed as β-sheets [43]. No such increase in dissipation was recorded during adsorption of S-WLBU2 at low concentration (Figure 7, bottom right), suggesting that there is no significant α-helix → β-sheet transition of S-WLBU2 within the PEO layer. The QCM-D results of Figure 7 are entirely consistent with the other results discussed above, and are also in agreement with the hypothesis that highly-elutable coiled-coil structures are formed at high peptide densities in the PEO brush.

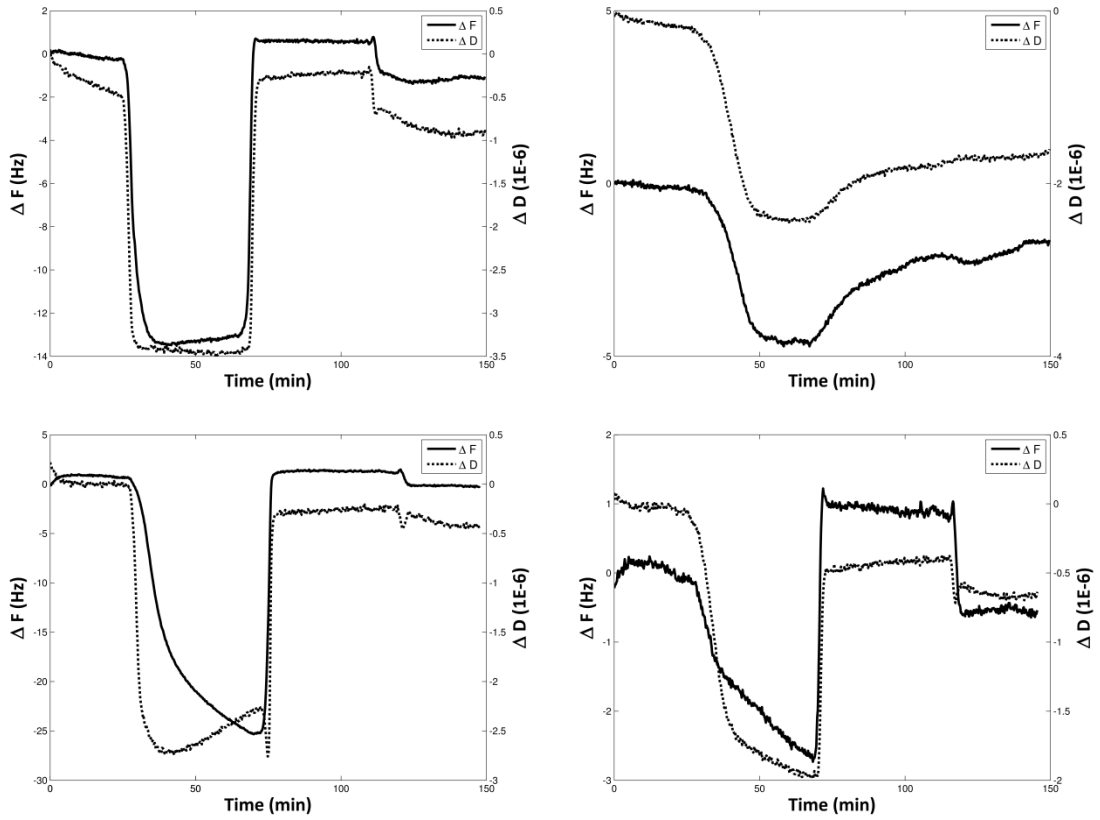

Figure 7. Representative Δ*F* and Δ*D* vs. time for WLBU2 (top panels) and S-WLBU2 (bottom panels) adsorption and elution on F108-coated SiO_2 QCM-D sensors. Baselines were achieved using 0.2 M $HClO_4$, followed by introduction of peptide in $HClO_4$, then elution with H_2O, and finally switch back to $HClO_4$. Peptide concentrations used for QCM-D experiments were 0.1 mg/mL (left panels) and 0.005 mg/mL (right panels). Note change of scale between peptide concentrations (left and right panels).

Conclusions

Elution of peptides from PEO brush layers is governed by their amphiphilicity and surface density. Peptides of high amphiphilicity can be expected to interact strongly with PEO chains after location within the layer, thus promoting their resistance to elution. However, at sufficiently high surface density, peptide-peptide interactions may result in conformational changes (e.g. formation of coiled-coils) which can compromise this resistance to elution. In this work, WLBU2, a peptide with a face-segregated amphiphilic α-helical structure, was observed to form α-helices and coiled-coils, while the amphiphilic peptide (S-WLBU2) with a more uniform charge distribution formed β-sheets. These conformational changes (from α-helix to coiled-coil and β-sheet) increased the elutability of WLBU2 and S-WLBU2, presumably by reducing the amphiphilic character of the resulting complex. In contrast, the non-amphiphilic peptide (PLR) showed no substantial change in structure or elutability with increasing peptide surface density. Entrapment of bioactive peptides within otherwise non-fouling PEO brush layers holds promise for contributing to development of responsive drug delivery systems. These results will inform research efforts focused on the sequential and competitive adsorption and release of such peptides at PEO layers. They will also be valuable for development of systems to control the rate and extent of therapeutic peptide release from PEO layers, based on modulation of their amphiphilicity and surface density.

Acknowledgments

The authors thank Dr. Kerry McPhail of the OSU College of Pharmacy for use of her CD instrument. This work was supported in part by the National Institute of Biomedical Imaging and Bioengineering (NIBIB, Grant No. R01EB011567). The content is solely the responsibility of

the authors and does not necessarily represent the official views of NIBIB or the National Institute of Health.

References

[1] X. Wu, M.P. Ryder, J. McGuire and K.F. Schilke, Adsorption, structural alteration and elution of peptides at pendant PEO layers, Colloids Surf. B. Biointerfaces, 112 (2013) 23-29.

[2] F. Costa, I.F. Carvalho, R.C. Montelaro, P. Gomes and M.C.L. Martins, Covalent immobilization of antimicrobial peptides (AMPs) onto biomaterial surfaces, Acta Biomater., 7 (2011) 1431-1440.

[3] B. Deslouches, I.A. Gonzalez, D. DeAlmeida, K. Islam, C. Steele, R.C. Montelaro and T.A. Mietzner, *De novo*-derived cationic antimicrobial peptide activity in a murine model of Pseudomonas aeruginosa bacteraemia, J. Antimicrob. Chemother., 60 (2007) 669-672.

[4] B. Deslouches, K. Islam, J.K. Craigo, S.M. Paranjape, R.C. Montelaro and T.A. Mietzner, Activity of the *de novo* engineered antimicrobial peptide WLBU2 against *Pseudomonas aeruginosa* in human serum and whole blood: Implications for systemic applications, Antimicrob. Agents Chemother., 49 (2005) 3208-3216.

[5] B. Deslouches, S.M. Phadke, V. Lazarevic, M. Cascio, K. Islam, R.C. Montelaro and T.A. Mietzner, *De novo* generation of cationic antimicrobial peptides: Influence of length and tryptophan substitution on antimicrobial activity, Antimicrob. Agents Chemother., 49 (2005) 316-322.

[6] I.A. Gonzalez, X.X. Wong, D. De Almeida, R. Yurko, S. Watkins, K. Islam, R.C. Montelaro, A. El-Ghannam and T.A. Mietzner, Peptides as potent antimicrobials tethered to a solid surface: Implications for medical devices, Nature Precedings, (2008).

[7] S.A. Onaizi and S.S.J. Leong, Tethering antimicrobial peptides: Current status and potential challenges, Biotechnol. Adv., 29 (2011) 67-74.

[8] M.C. Skinner, A.O. Kiselev, C.E. Isaacs, T.A. Mietzner, R.C. Montelaro and M.F. Lampe, Evaluation of WLBU2 peptide and 3-*O*-octyl-*sn*-glycerol lipid as active ingredients for a topical microbicide formulation targeting *Chlamydia trachomatis*, Antimicrob. Agents Chemother., 54 (2010) 627-636.

[9] A.A. Adzhubei, M.J.E. Sternberg and A.A. Makarov, Polyproline-II Helix in Proteins: Structure and Function, J. Mol. Biol., 425 (2013) 2100-2132.

[10] B. Bochicchio and A.M. Tamburro, Polyproline II structure in proteins: Identification by chiroptical spectroscopies, stability, and functions, Chirality, 14 (2002) 782-792.

[11] A.V. Mikhonin, N.S. Myshakina, S.V. Bykov and S.A. Asher, UV Resonance Raman Determination of Polyproline II, Extended 2.5_1-Helix, and β-Sheet Ψ Angle Energy Landscape in Poly-*L*-Lysine and Poly-*L*-Glutamic Acid, J. Am. Chem. Soc., 127 (2005) 7712-7720.

[12] J.M. Rifkind, Helix–coil transition of poly-L-arginine: A comparison with other basic polypeptides, Biopolymers, 8 (1969) 685-688.

[13] M.L. Tiffany and S. Krimm, Circular dichroism of the "random" polypeptide chain, Biopolymers, 8 (1969) 347-359.

[14] W.H. DeJohng and P.J.A. Borm, Drug delivery and nanoparticles: Applications and hazards, Int. J. Nanomed., 3 (2008) 133-149.

[15] S.-D. Li and L. Huang, Pharmacokinetics and biodistribution of nanoparticles, Mol. Pharm., 5 (2008) 496-504.

[16] T.R. Pisanic, 2nd, J.D. Blackwell, V.I. Shubayev, R.R. Finones and S. Jin, Nanotoxicity of iron oxide nanoparticle internalization in growing neurons, Biomaterials, 28 (2007) 2572-2581.

[17] M.P. Ryder, K.F. Schilke, J.A. Auxier, J. McGuire and J.A. Neff, Nisin adsorption to polyethylene oxide layers and its resistance to elution in the presence of fibrinogen, J. Colloid Interface Sci., 350 (2010) 194-199.

[18] K.F. Schilke and J. McGuire, Detection of nisin and fibrinogen adsorption on poly (ethylene oxide) coated polyurethane surfaces by time-of-flight secondary ion mass spectrometry (TOF-SIMS), J. Colloid Interface Sci., 358 (2011) 14-24.

[19] R.H. MuÈller, K. MaÈder and S. Gohla, Solid lipid nanoparticles (SLN) for controlled drug delivery–a review of the state of the art, Eur. J. Pharm. Biopharm., 50 (2000) 161-177.

[20] X. Huang and C.S. Brazel, On the importance and mechanisms of burst release in matrix-controlled drug delivery systems, J. Controlled Release, 73 (2001) 121-136.

[21] M.C. Lampi, X. Wu, K.F. Schilke and J. McGuire, Structural attributes affecting peptide entrapment in PEO brush layers, Colloids Surf. B. Biointerfaces, 106 (2013) 79-85.

[22] Y.-C. Tai, J. McGuire and J.A. Neff, Nisin antimicrobial activity and structural characteristics at hydrophobic surfaces coated with the PEO–PPO–PEO triblock surfactant Pluronic® F108, J. Colloid Interface Sci., 322 (2008) 104-111.

[23] J.K. Dill, J.A. Auxier, K.F. Schilke and J. McGuire, Quantifying nisin adsorption behavior at pendant PEO layers, J. Colloid Interface Sci., 395 (2013) 300-305.

[24] H. Lee, D.H. Kim, K.N. Witte, K. Ohn, J. Choi, B. Akgun, S. Satija and Y.-Y. Won, Water Is a Poor Solvent for Densely Grafted Poly(ethylene oxide) Chains: A Conclusion Drawn from a Self-Consistent Field Theory-Based Analysis of Neutron Reflectivity and Surface Pressure–Area Isotherm Data, J. Phys. Chem. B, 116 (2012) 7367-7378.

[25] D.A.D. Parry, R.D.B. Fraser and J.M. Squire, Fifty years of coiled-coils and α-helical bundles: A close relationship between sequence and structure, J. Struct. Biol., 163 (2008) 258-269.

[26] N.E. Zhou, C.M. Kay and R.S. Hodges, Synthetic model proteins. Positional effects of interchain hydrophobic interactions on stability of two-stranded α-helical coiled-coils, J. Biol. Chem., 267 (1992) 2664-2670.

[27] N.E. Zhou, C.M. Kay and R.S. Hodges, Synthetic model proteins: the relative contribution of leucine residues at the nonequivalent positions of the 3-4 hydrophobic repeat to the stability of the two-stranded α-helical coiled-coil, Biochemistry (Mosc). 31 (1992) 5739-5746.

[28] G. Grigoryan and A.E. Keating, Structural specificity in coiled-coil interactions, Curr. Opin. Struct. Biol., 18 (2008) 477-483.

[29] B. Rubinov, N. Wagner, H. Rapaport and G. Ashkenasy, Self-replicating amphiphilic beta-sheet peptides, Angew. Chem. Int. Ed. Engl., 48 (2009) 6683-6686.

[30] K. Wang, J.D. Keasling and S.J. Muller, Effects of the sequence and size of non-polar residues on self-assembly of amphiphilic peptides, Int. J. Biol. Macromol., 36 (2005) 232-240.

[31] N.J. Greenfield, Methods to estimate the conformation of proteins and polypeptides from circular dichroism data, Anal. Biochem., 235 (1996) 1-10.

[32] N.J. Greenfield and G.D. Fasman, Computed circular dichroism spectra for the evaluation of protein conformation, Biochemistry (Mosc). 8 (1969) 4108-4116.

[33] L. Whitmore and B.A. Wallace, DICHROWEB, an online server for protein secondary structure analyses from circular dichroism spectroscopic data, Nucleic Acids Res., 32 (2004) W668-W673.

[34] L. Whitmore and B.A. Wallace, Protein secondary structure analyses from circular dichroism spectroscopy: Methods and reference databases, Biopolymers, 89 (2008) 392-400.

[35] T.M. Cooper and R.W. Woody, The effect of conformation on the CD of interacting helices: a theoretical study of tropomyosin, Biopolymers, 30 (1990) 657-676.

[36] R. Cukalevski, M. Lundqvist, C. Oslakovic, B. Dahlback, S. Linse and T. Cedervall, Structural changes in apolipoproteins bound to nanoparticles, Langmuir, 27 (2011) 14360-14369.

[37] F. Fiumara, L. Fioriti, E.R. Kandel and W.A. Hendrickson, Essential role of coiled coils for aggregation and activity of Q/N-rich prions and polyQ proteins, Cell, 143 (2010) 1121-1135.

[38] N.D. Lazo and D.T. Downing, Circular Dichroism of Model Peptides Emulating the Amphipathic α-Helical Regions of Intermediate Filaments, Biochemistry (Mosc). 36 (1997) 2559-2565.

[39] S.A. Potekhin, T.N. Melnik, V. Popov, N.F. Lanina, A.A. Vazina, P. Rigler, A.S. Verdini, G. Corradin and A.V. Kajava, De novo design of fibrils made of short α-helical coiled coil peptides, Chem. Biol., 8 (2001) 1025-1032.

[40] J.P. Schneider and J.W. Kelly, Templates that induce α-helical, β-sheet, and loop conformations, Chem. Rev., 95 (1995) 2169-2187.

[41] F. Höök, B. Kasemo, T. Nylander, C. Fant, K. Sott and H. Elwing, Variations in Coupled Water, Viscoelastic Properties, and Film Thickness of a Mefp-1 Protein Film during Adsorption and Cross-Linking: A Quartz Crystal Microbalance with Dissipation Monitoring, Ellipsometry, and Surface Plasmon Resonance Study, Anal. Chem., 73 (2001) 5796-5804.

[42] F. Höök, J. Vörös, M. Rodahl, R. Kurrat, P. Böni, J.J. Ramsden, M. Textor, N.D. Spencer, P. Tengvall, J. Gold and B. Kasemo, A comparative study of protein adsorption on titanium oxide surfaces using in situ ellipsometry, optical waveguide lightmode spectroscopy, and quartz crystal microbalance/dissipation, Colloids Surf. B. Biointerfaces, 24 (2002) 155-170.

[43] M. Binazadeh, H. Zeng and L.D. Unsworth, Effect of peptide secondary structure on adsorption and adsorbed film properties on end-grafted polyethylene oxide layers, Acta Biomater., 10 (2014) 56-66.

[44] M.V. Voinova, M. Jonson and B. Kasemo, 'Missing mass' effect in biosensor's QCM applications, Biosensors Bioelectron., 17 (2002) 835-841.